OPTICAL DESIGN OF THE ELECTRON PULSE STRETCHER FACILITY AmPS

R. Maas and Y.Y. Wu

NIKHEF-K, P.O. Box 41882, 1009 DB Amsterdam, The Netherlands

Abstract

AmPS is a 900 MeV electron Pulse Stretcher / Storage ring which is expected to become operational during 1992. In Stretcher Mode a 2.1 μs beam pulse of 80 mA peak current is injected during three turns into the 211.6 m long ring. Injection frequency is 400 Hz. Two fast electrostatic deflectors (fall time < 80 ns) are used to displace the closed orbit (C.O.) prior to injection; at the end of the injection cycle the C.O. is restored. The RF system consists of a 2856 MHz travelling wave structure. Phase modulation of the RF, together with the synchrotron loss, is used to extract the beam utilizing the third integer resonance ($\nu_x = 8.30$). Simulations indicate a clean extraction ($i_{av} = 50\ \mu A$) without excessive demands on the RF system.
For operation in Storage Mode (i = 200 mA), AmPS will be equipped with an internal target facility. A second RF system, operating at f = 500 MHz, will be used in this mode of operation.

AmPS Stretcher

General description

In Fig. 1 the layout of the ring, plus the various beam lines around it, is given. Not shown are the linac proper and the ESC (Energy Spectrum Compressor), placed after the linac. The emerging beam from the ESC enters B_1, see Fig. 1. It is possible to deliver a (low-duty factor) beam directly onto the EMIN target area via the complete Beam Switch Yard (BSY) B_1,...,B_2,..,B_3,..,B_4,..,B_5, ..,'target', thus bypassing the Stretcher. Injection into AmPS utilizes the first part of the BSY: B_1,..,B_2,..,B_6,...,'Injection'.

The extracted beam proceeds via B_7,..,B_8,..,(B_3)...,B_4,..,B_5, ..,'target'. The level of the ring is 1.45 m, while the level of both the linac and BSY is 1.30 m, so there is little interference between the various lines. The only 'real' crossing is the line emerging from B_4, and the line entering B_6, see Fig. 1.
The ring comprises four curved sections, connected by four straights. Each curved section comprises four cells (Fig. 2) with $\nu_x = \nu_y = 0.25$, so the four cells form an achromat. Two families of sextupoles, S_h and S_v, control the chromaticity ($\chi_x^{nat} = -9.4$;

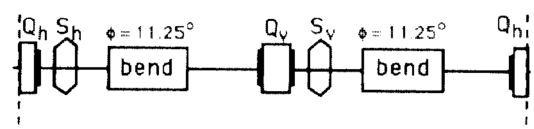

Fig. 2 Structure of one-quarter of a curved section. Q is quadrupole, S is sextupole; h/v: horizont./vert.

$\chi_y^{nat} = -9.5$). The curved section can be tuned as a second-order achromat [1]. Each straight section consists of two so-called 'matching' cells, which are each others mirror image. This ensures proper matching of the curved sections, since all α's (Twiss parameter) at both the beginning and end of each matching cell are zero. The beta functions in the straights reach a maximum in the centre, Fig. 3. The physical layout (quadrupole position) of each of the four straights is identical; however, in the east-straight (called the Injection straight) the β_x function reaches a maximum value of 25 m, while in the other three straights the maximum value of β_x is 16.5 m. In this way the beam oscillations during extraction can be reduced (by roughly $\sqrt{[16.5/25]}$) in most parts of the machine (except of course the injection area).

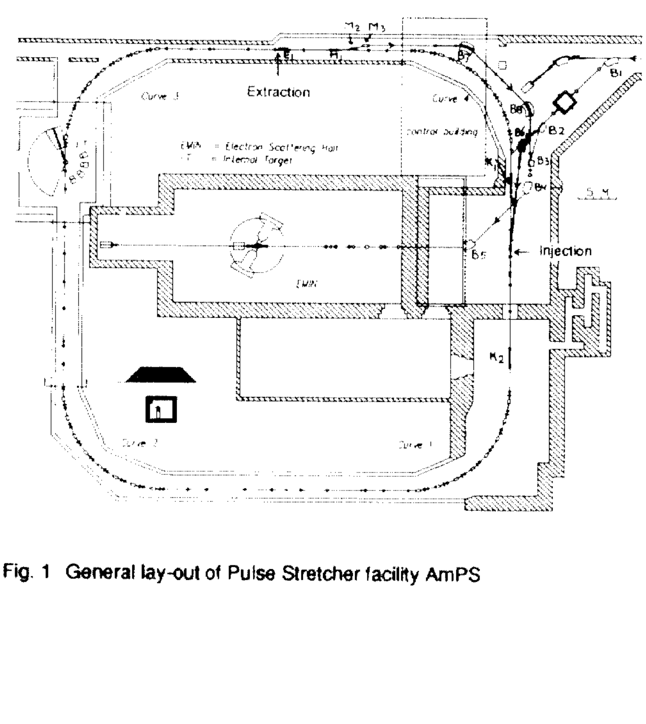

Fig. 1 General lay-out of Pulse Stretcher facility AmPS

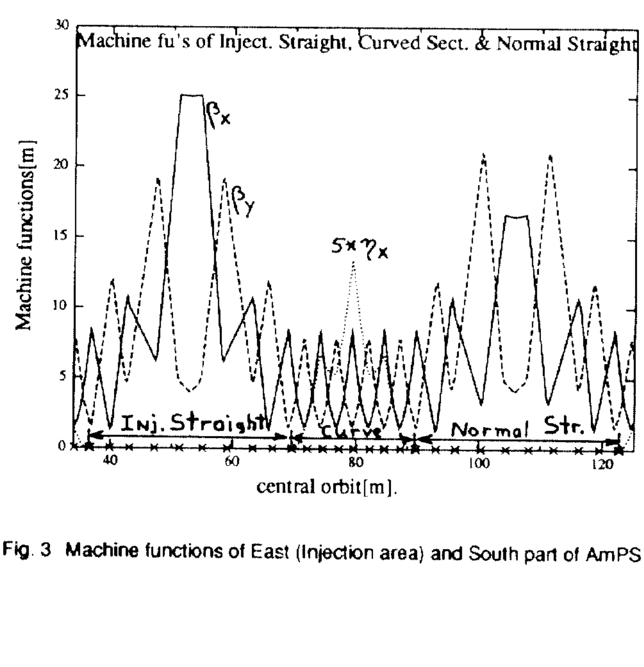

Fig. 3 Machine functions of East (Injection area) and South part of AmPS

Injection

The beam is injected from below into the horizontal phase space (i.e. x–x') of the machine. The operating point is close to the third–order resonance: $\nu_x = 8.30$. Injection will take place over (almost) three turns. In order to avoid the recurring beam hitting the injection septum after the third turn, two fast electrostatic kickers (K_1, K_2, Fig. 1) displace the closed orbit (C.O.) vertically ($\Delta y = -15$ mm) prior to injection. After a flat top of 2.0 µs (corresponding to 2.8 turns) the injection process is terminated and the C.O. is restored fast (< 80 ns). The beam will then pass overhead the injection septum, Fig. 4. This septum is a one–winding DC type magnet with a septum thickness of 3 mm and a deflecting angle of 16.2 mrad. At E = 900 MeV the current is 1000 A, producing a field of 1.2 kG.
In the (x–x')–plane the injection occurs off–axis ($\Delta x = 15.8$ mm) in order to create in the (x–x') *phase space* a hollow beam; this feature allows complete extraction (see below) of the beam from the machine, before the next injection pulse arrives. The large value of the chromaticity ($\chi_x = -15$), combined with the energy spread of the injected beam ($\delta E/E = \pm$ 0.05%) leads to a rapid spread of the injected beam over the available (hollow) area: simulations show that after 100 turns the distribution in the hollow area is essentially uniform.

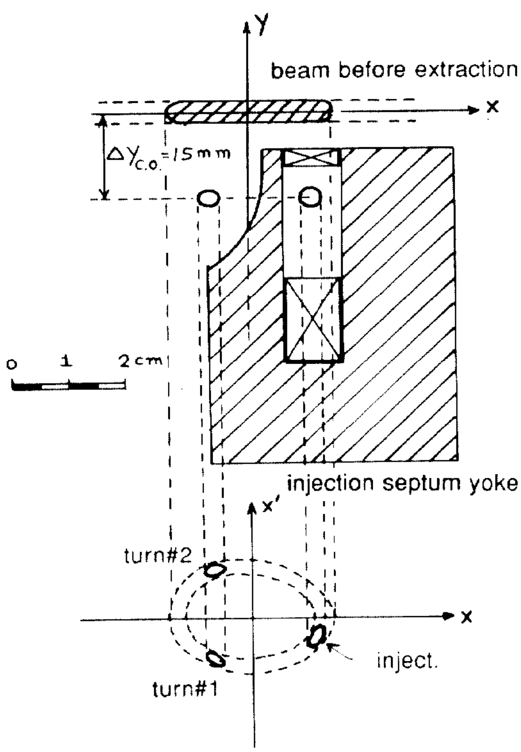

Fig. 4 Geometry of magnetic injection septum. Top part shows situation in *real* space; bottom part shows (x, x') *phase space* at injection location.

Extraction

The lay–out of the extraction line is given in Fig. 1. The beam is extracted by an electrostatic foil septum, E_1. Some important parameters of this septum are: L = 0.90 m; g = 40 kV/cm; foil thickness 50 µm; deflecting angle 4.0 mrad. The extracted beam then first traverses two ring quads before it is deflected out of the machine by a magnetic septum magnet, M_1 . This septum is of similar type as the injection septum (L = 0.69 m; defl. angle 65 mrad; septum thickness 6 mm; B = 2.8 kG @ I_{max} = 2250 A). The beam is shifted laterally over 0.70 m by two conventional 20°–dipoles of opposite polarity before it enters the 90°–bend section. This section comprises two 45°–dipoles (B_7 and B_8), two quads in the centre, and two quads on either side of the section. The section is a unit transform in both transverse planes (T_x = I; T_y = –I). The emerging beam from this section is fed into the second part of the BSY, starting with B_4 (B_3 is switched off). In order to create the proper matching conditions between extracted beam and BSY, a (4—quadrupole) matching section is located between M_1 and the 90°–bend section.

For the extraction process the third–integer resonance is used. The necessary non-linearity which drives the resonance is provided by 4 sextupoles, one in each (dispersion-free) straight section. During the extraction the tune is kept constant, i.e. no pulsed quadrupoles are used. A large value of the chromaticity ($\chi_x = -15$), combined with an energy loss mechanism (synchrotron radiation), see below, provides the mechanism to slowly push the beam into the unstable part of the phase space (monochromatic extraction). Extraction simulations show that the orientation of the triangular separatrix (in x–x' phase space) can be manipulated to some extent by using a different strength for each extraction sextupole. Typical values of sextupole strengths k_s are (sex2, sex3, sex4 – only three of the four are used):
k_s = (–/–/+) 4.8 m^{-3}. The length of each sextupole is 0.2 m, so the total (integrated) sextupole strength K_s is K_s = 2.9 m^{-2}. Using all four extraction sextupoles (keeping the value of K_s fixed) yields an almost identical result; however, if the total strength K_s is generated by only one sextupole, chaotic motion can be observed.

In order to compensate for the synchrotron losses (U_0=17.6 keV/rev at E = 900 MeV), *and* to control the extraction process, a 2856 MHz travelling wave RF cavity system will be installed. We plan to slowly extract the beam by phase–modulating the RF voltage ,thereby slowly spilling the particles out of the RF bucket. Simulation results of this technique are given in [2]; practical results have been reported in [3].

Orbit correction

The orbit correction (O.C.) scheme comprises 32 combined x–y steering coils and 32 stripline monitors. Both the curved sections and the straight sections contain each 4 corrector / stripline units; The maximum deflection angle (in both transverse planes) of each corrector is 1 mrad. (at E = 1 GeV). In order to test the scheme, the following misalignments (Gaussian distribution, truncated at 1σ) were assumed:

quad's/sextupoles: $\Delta x = \Delta y = 0.2$ mm; $\Delta\phi = 1.0$ mrad.
dipoles: $\Delta x = \Delta y = 0.2$ mm; $\Delta\phi = 0.3$ mrad; $\delta B/B = 2\times10^{-4}$
monitors: $\Delta x = \Delta y = 0.2$ mm; reading errors: $\Delta x = \Delta y = 0.25$ mm.
Fig. 5 shows both the uncorrected closed orbit (C.O.), and the C.O. after correction (results obtained by MAD [4]). Corrector values are, depending on the particular set of misalignments, generally below 0.5 mrad.

In addition to the 32 stripline monitors, 16 viewscreens will be installed: two screens in each curved section, and two in each straight. The location of the screens has been chosen such that beam position information from them can be used for a 'minor' orbit correction scheme (utilizing only 16 out of the available 32 steering coils).

In three selected area's, (RF cavity, Injection Area and Extraction Area) it is possible to use the four closest corrector coils to create a local orbit bump $(z, z')_{z=x,y}$. This feature allows a very local correction of the C.O. Since the bump and the 'normal' O.C. are

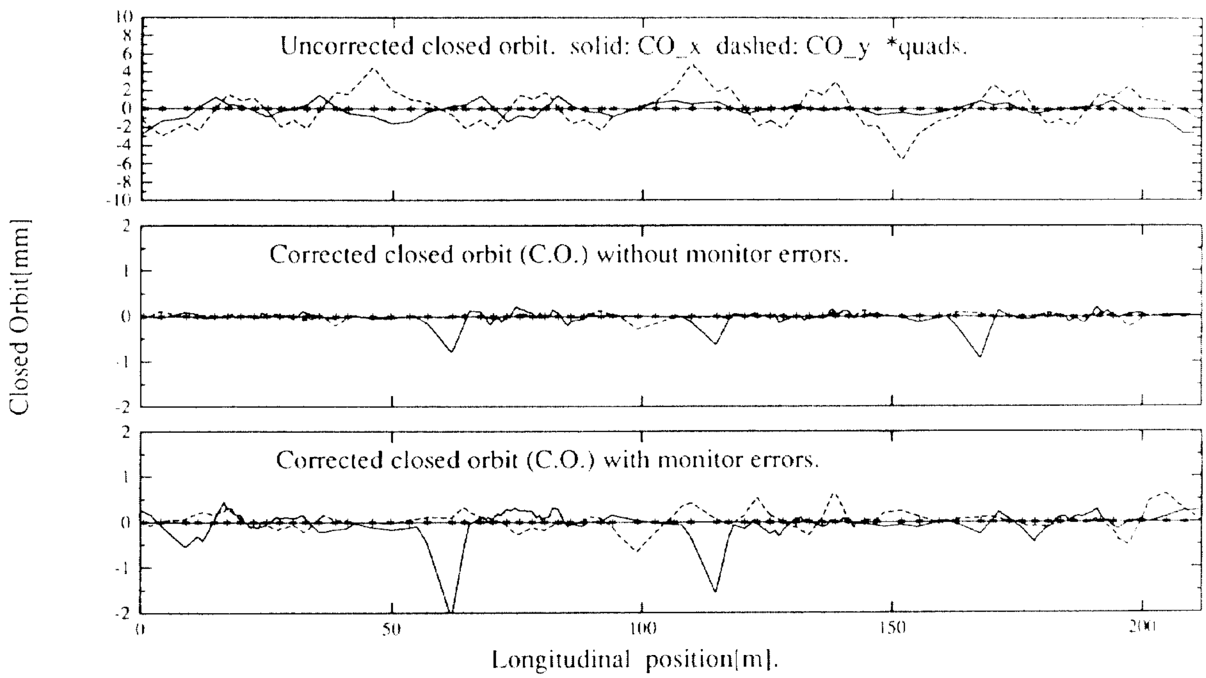

Fig. 5 Orbit correction and misalignment errors (numbers in text): Top: UNcorrected closed orbit (C.O.)
Middle: Corrected C.O. without misaligned monitirs and reading errors. Bottom: Corrected C.O. including misaligned monitors and reading errors

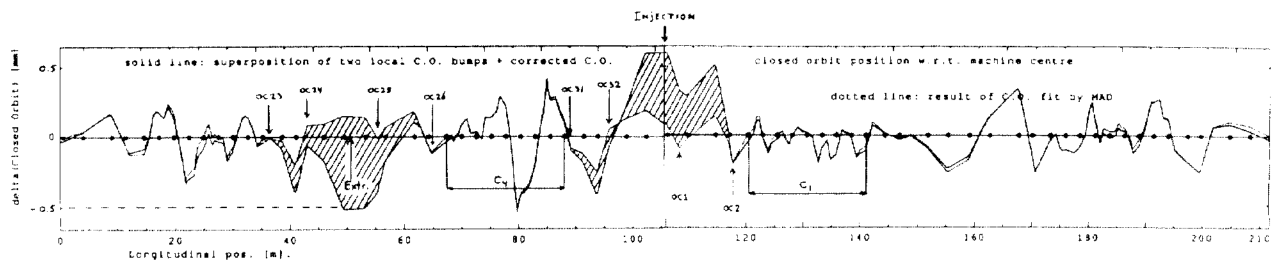

Fig. 6 Two local bumps superimposed on corrected Closed Orbit (C.O.). Dotted line: original C.O. trajectory; solid line: new C.O. resulting from new corrector settings (eight in total) around the two bump area's.

linear superpositions, the local bump does not influence the O.C. scheme, although the same corrector coils are used. Only the maximum power rating of the coils should not be exceeded. Fig. 6 shows two additional local bumps: one ($\Delta x = 0.5$ mm, $\Delta x' = 0.0$ mrad at the Injection point), created by coils OC31, OC32, OC1 and OC2, and one ($\Delta x = -0.5$ mm, $\Delta x' = 0.0$ mrad at the Extraction point), created by coils OC23, OC24, OC25 and OC26. Fig. 6 shows that the trajectory of the corrected C.O. remains essentially unchanged outside the two bump area's, although in this case eight O.C. coils have a different setting.

sextupole components of dipoles and steering coils

The total (integrated) sextupole strength of the extraction sextupoles is typically of the order of $K_s \sim 3\ m^{-2}$, as has been mentioned above. The sextupole component of the steering coil field (160 G @ E = 900 MeV for l = 0.2 m) in the x–x' plane, therefore, should be small compared to this, since otherwise the extraction process will be difficult to control. If we, arbitrarily, demand that the total sextupole contribution from the 16 steering coils in the straight sections should not exceed 2 % of K_s, then the radial inhomogeneity of the field over a range x = ± 5 cm, should not exceed 1 %. Since the extraction process occurs in the x-x' plane, one can relax the tolerances for the sextupole component in the y–plane somewhat. A design for such a (window frame) steering coil is being made at this moment.

The sextupoles in the curved sections are used to control the chromaticity. In order to produce $\chi_x = -15$ and $\chi_y = +0.2$, the following sextupole strengths are required (Fig. 2):
$K_s(S_h) = -0.15\ m^{-2}$; $K_s(S_v) = -0.65\ m^{-2}$.
In order to assess the effects of spurious sextupole strength in the curved sections, we assumed each dipole possesses an integrated sextupole strength of $-0.1\ m^{-2}$. Then the chromaticity was re-fitted. Extraction simulations showed only a small change in the orientation of the triangular separatrix. This relative insensitivity to spurious sextupole strength is probably due to the symmetric lay–out of the curved section (Fig. 2).

[1] K.L. Brown, SLAC–PUB–2257 (Feb. 1979).
[2] R. Maas and Y.Y. Wu, Proceedings of the 1989 IEEE Particle Accelerator Conference, Chicago, IL, 1989, pp. 1698–1700.
[3] L.O. Dallin, SAL Report No. 38, (thesis), 1990,
[4] The MAD Program, Version 7.2, F. C. Iselin and J. Niederer, CERN / LEP–TH / 88–38